ELLIPTIC RELAXATION SECOND MOMENT CLOSURE FOR TURBULENT HEAT FLUX

Jong Keun Shin
Department of Automotive Engineering, Donghae University,
119, Jiheung-dong, Donghae, Kangwondo 240-713, Korea
jkshin@donghae.ac.kr

Jeong Soo An, Young Don Choi
Department of Mechanical Engineering, Korea University,
1, Anam-dong, Sungbuk-ku, Seoul 136-701, Korea
anjsoo@korea.ac.kr, ydchoi@korea.ac.kr

ABSTRACT

The present contribution describes the development of near-wall second moment turbulent heat flux closure and its application to turbulent flows rotating with heat transfer to test the performance of the model. The second-moment models for turbulent heat fluxes are proposed on the basis of elliptic concept. The new models satisfy the near-wall balance between viscous diffusion, viscous dissipation and temperature-pressure gradient correlation, and also have the characteristics of approaching its respective conventional high Reynolds number model far away from the wall. In order to develop the new heat flux models, first of all, the velocity field variables are supplied from the DNS data, and the differential equations only for the mean temperature and the scalar flux are solved by the present calculations with constant wall heat flux and constant wall temperature boundary conditions respectively. And then, the rotating channel and square duct flows with heat transfer have been simulated by the present heat flux models. The predictions in rotating and non-rotating flows show that the behavior of the turbulent heat transfer in the whole flow region is well captured by the present models.

INTRODUCTION

In the engineering applications, various types of thermal boundary conditions can be imposed on the velocity field. It is thus necessary to obtain the practically important quantities, such as the turbulent heat flux and the heat transfer coefficient (Nagano & Hattori, 2003). The most common approach to turbulent heat transfer studies is to model the normal heat flux using the classical Boussinesq approximation. The researchers try to improve the modelling by turning to two-equation and algebraic flux model for heat transport. Despite some success, it is still believed that the most reliable prediction methods are those based on a second moment closure (Lai & So, 1990). Although much progress has been achieved in the modelling of the Reynolds stress transport equations with the elliptic concept, the second moment modelling of the scala field, on the other hand, is rather primitive. The reason is that turbulent stresses directly affect the heat flux equations. Therefore, the development of second moment heat flux closure depends largely on the availability and correctness of the Reynolds stress model. For the turbulent stress field, Durbin(1993) and Thielen *et al.*(2005) introduced new type of wall blocking model known as the elliptic relaxation equation(ERE) and elliptic blending model(EBM) respectively. A notable feature of these approaches is that the non-local character is preserved through the elliptic operator, and the formulation can be integrated down to the wall.

The objective of the present study is extension of the elliptic operator to full second-moment treatment of the heat flux. Therefore, the present approach for the turbulent heat flux modeling is similar to those of ERE and EBM, and is based on the limiting wall behaviour of the heat flux transport equations. The proposed model is validated against fully-developed channel flow DNS data with constant wall heat flux and constant wall temperature difference boundary conditions respectively. And then, the rotating channel and square duct flows with heat transfer have been simulated by the present heat flux models. The elliptic-blending second-moment turbulence closure has been essentially utilized to calculate the realistic rotating flow fields. The results of prediction are directly compared to the DNS and the LES to assess the performance of the model predictions.

MATHEMATICAL MODELS

Elliptic blending equation turbulent heat flux model

A mathematical model of turbulent scalar transport is required for solving the Reynolds-averaged scalar equation. In the second moment closure, the generation term due to mean velocity and scalar gradients can be handled exactly, and this feature should be one of the most attractive advantages when predicting complex flows. When the buoyancy effect can be neglected, the transport equation for the scalar flux in a fluid of constant physical properties is given as:

$$\frac{D\overline{u_i\theta}}{Dt} = P_{i\theta} + F_{i\theta} + D^t_{i\theta} + D^\nu_{i\theta} + \Phi^*_{i\theta} - \epsilon_{i\theta} \qquad (1)$$

The meaning of the terms in equation (1) from left to right are convective transport, production terms of turbulent heat flux, Coriolis term, turbulent diffusive transport, viscous diffusive transport, pressure scrambling (temperature-pressure gradient correlation) and molecular dissipation of heat fluxes. Considering the near-wall behaviour of heat flux equations, the unclosed terms in Eq. (1) can be modelled as follows. Firstly, the turbulent diffusion term in Eq. (1) is modelled via the standard gradient transport hypothesis as:

$$D_{i\theta}^{t} = \frac{\partial}{\partial x_k}\left(C_\theta \overline{u_k u_l}\, T \frac{\partial \overline{u_i\theta}}{\partial x_l} \right) \tag{2}$$

with the coefficient $C_\theta = 0.153$. Contrary to the Reynolds stress model, the molecular diffusion is not of the correct term. The model suggested by Lai & So(1990) is adopted as:

$$D_{i\theta}^{\nu} = \nu \frac{\partial^2 \overline{u_i\theta}}{\partial x_k^2} + \frac{\alpha-\nu}{n_i+2} \frac{\partial^2 \overline{u_i\theta}}{\partial x_k^2} \text{(no summation for } i\text{)} \tag{3}$$

In Eq. (3), the n_i means the unit normal to the wall. The temperature-pressure gradient correlation term $\Phi_{i\theta}^{*}$ and the dissipation term $\epsilon_{i\theta}$ are major sink term and need to be carefully modeled. By following the same approach as for the turbulent stress field, we can express the pressure scrambling and molecular destruction with elliptic equations analogue to EBM:

$$\Phi_{i\theta}^{*} = (1-\psi^2)\Phi_{i\theta}^{w} + \psi^2 \Phi_{i\theta}^{h} \tag{4}$$

$$\epsilon_{i\theta} = (1-\psi^2)\epsilon_{i\theta}^{w} + \psi^2 \epsilon_{i\theta}^{h} \tag{5}$$

In the above models, the ellipticity of the models is preserved by solving an elliptic differential equation as

$$\psi - L^2 \nabla^2 \psi = 1 \tag{6}$$

with the boundary conditions $\psi = 0$ at the wall (Thielen *et al.*, 2005). For $\Phi_{i\theta}^{h}$ any known quasi-homogeneous model can be adopted and the most general model (Durbin, 1993) is chosen in the present study.

$$\Phi_{i\theta}^{h} = -C_{1\theta}\frac{\epsilon}{k}\overline{u_i\theta} + C_{2\theta}\overline{u_i u_j}\frac{\partial \Theta}{\partial x_j} + C_{3\theta}\overline{u_j\theta}\frac{\partial U_i}{\partial x_j} \tag{7}$$

with $C_{1\theta} = 2.5$, $C_{2\theta} = 0.45$ and $C_{3\theta} = 0.0$. Because the dissipation term in the high Reynolds number region has been assumed to be isotropic, we let

$$\epsilon_{i\theta}^{h} = 0. \tag{8}$$

To impose the limiting wall behaviour of turbulent heat fluxes, $\Phi_{i\theta}^{w}$ and $\epsilon_{i\theta}^{w}$ can be modeled in such a way that it will approach its asymptotic value near the wall.

$$\Phi_{i\theta}^{w} = -\frac{\epsilon}{k}\overline{u_k\theta}\, n_k n_i \tag{9}$$

$$\epsilon_{i\theta}^{w} = \frac{1}{2}\left(1+\frac{1}{\mathrm{Pr}}\right)\frac{\epsilon}{k}\left(\overline{u_i\theta} + \overline{u_k\theta}\, n_k n_i\right) \tag{10}$$

For the reproduction of the limiting wall behaviour of $\Phi_{i\theta}^{w}$ and $\epsilon_{i\theta}^{w}$, the wall-normal vector is used. However, the use of a wall-normal vector must be avoided, since such a quantity is often not well defined in complex geometries. Therefore, in the present work, a new concept suggested by Thielen *et al.*(2005) is adopted as:

$$\mathbf{n} = \frac{\nabla \psi}{\| \nabla \psi \|} \tag{11}$$

Elliptic relaxation equation turbulent heat flux model

In order to introduce the elliptic relaxation concept originated from Durbin(1993) in the second moment turbulent heat flux closure, the pressure scrambling can be expressed as:

$$\Phi_{i\theta}^{*} = k f_{i\theta} \tag{12}$$

In the above model, $f_{i\theta}$ is obtained from the elliptic relaxation equation as:

$$f_{i\theta} - L^2 \nabla^2 f_{i\theta} = \mathcal{L}(f_{i\theta}) \tag{13}$$

where,

$$\mathcal{L}(f_{i\theta}) = \frac{1}{k}\left[\Phi_{i\theta}^{h} + \frac{1}{2}\left(1+\frac{1}{\mathrm{Pr}}\right)\frac{\epsilon}{k}\left(\overline{u_i\theta}\right)\right]. \tag{14}$$

For the homogeneous pressure scrambling model $\Phi_{i\theta}^{h}$, Durbin's model represented in Eq. (7) is adopted with the some modification in the model coefficient. The modified coefficient is $C_{1\theta}$, which is assigned to 2.0. The modification of the model coefficient is obtained against fully-developed channel flow DNS data with constant wall heat flux and constant wall temperature difference boundary conditions respectively. To impose the limiting wall behaviour of turbulent heat fluxes, the molecular dissipation rate can be modeled as follows.

$$\epsilon_{i\theta} = \frac{1}{2}\left(1+\frac{1}{\mathrm{Pr}}\right)\frac{\epsilon}{k}\left(\overline{u_i\theta}\right) \tag{15}$$

In equations (14) and (15), Pr means molecular Prandtl number. The wall boundary conditions for $f_{i\theta}$ are

$$f_{1\theta} = f_{3\theta} = 0,\ f_{2\theta} = -2\nu\left(1+\frac{1}{\mathrm{Pr}}\right)\frac{1}{y^2}\frac{\overline{u_i\theta}}{k}. \tag{16}$$

The equation (2), also, is adopted to the turbulent diffusion model in the elliptic relaxation second moment closure without any modification. On the other hand, in order to avoid using the wall-normal vector, the molecular diffusion is modeled as:

$$D_{i\theta}^{\nu} = \frac{(\alpha+\nu)}{2}\frac{\partial^2 \overline{u_i\theta}}{\partial x_k^2} \tag{17}$$

NUMERICAL TREATMENT

For the assesment of new second moment heat flux closures, the Reynolds-averaged Navier Stokes equation (RANS) simulation using the present heat flux models has been performed for the fully developed rotating channel and square duct flows with heat transfer. The computations for channel and square duct flows are carried out with a simple finite-volume solver and the majority of the grids is laid in the low Reynolds number region ($y^+ \le 70$) while the first grid is located at $y^+ = 0.1$. The Reynolds stresses, the heat fluxes and the mean velocities are set to 0 at the wall, and the wall dissipation rate is assigned to $\epsilon = 2\nu(\partial\sqrt{k}/\partial y)^2$.

RESULTS AND DISCUSSION

Development and calibration of new heat flux model

In order to develop and calibrate the new heat flux models, the velocity field variables are supplied from the DNS data, and the differential equations only for the mean temperature and the scalar flux are solved by the present calculations with constant wall heat flux and constant wall temperature difference boundary conditions

respectively. Therefore, any failure in the present models can be attributed to the heat flux modelling and two Reynolds number of $Re_\tau = 180$ and 395 are calculated, where Re_τ is based on the friction velocity u_τ and the channel half width $D/2$.

Profiles of mean temperature and heat fluxes in fully developed non-rotating channel flow with constant wall heat flux boundary condition are plotted in Fig. 1 compared to the DNS of Kawamura(2004) and Durbin's second moment heat flux model. Although Durbin's model does not use any near-wall approximations, but the profiles of wall-normal heat flux due to the model are well predicted surprisingly. In Fig. 1, EBE means the present elliptic blending equation second moment model and ERE the present elliptic relaxation equation model. In fully developed channel flows, because the mean temperature is affected by wall normal heat flux only, the profile of mean temperature due to Durbin's model is reasonably close to the DNS (Kawamura, 2004). On the other hand, this figure shows that the streamwise heat flux is globally well predicted by the present models. This result seems to be induced by the present near-wall models, which is introduced to consider the asymptotic proximity of heat fluxes in the near-wall region. However, it can be seen that the profiles of streamwise heat flux due to Durbin's model, which does not adopt any near wall model, is largely under-predicted in comparison with the DNS. In case of the predictions of the present EBE, the profile of Θ^+ is slightly under-estimated in the buffer region, but the profiles of heat fluxes are similar and reasonably close to the DNS. The distributions of temperature and heat fluxes due to the present ERE are most close to the DNS in comparison with the other models.

Figure 2 shows the distributions of temperature in fully developed channel flow with constant wall temperature boundary condition. From this result, we can see that the profiles of mean temperature are well predicted by the present elliptic concept models.

In order to determine the present model coefficients, we computed the non-rotating channel flows with heat transfer. The model coefficients taken from this calibration procedure should not have been altered for the imposed system rotation flows.

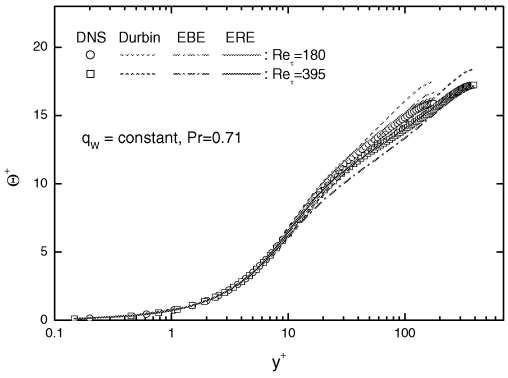

(a)

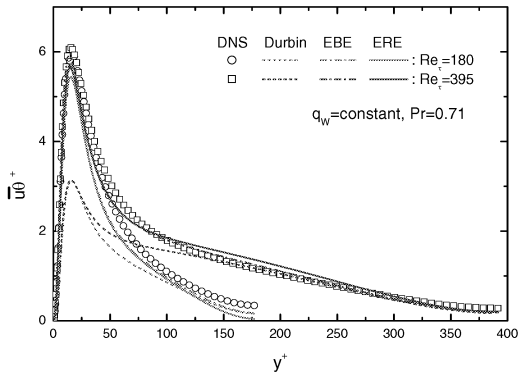

(b)

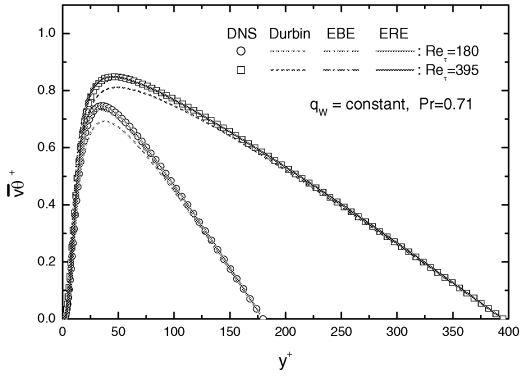

(c)

Fig. 1 Predicted heat transfer behaviour in a non-rotating channel with constant wall heat flux boundary condition. symbols: DNS(Kawamura, 2004), lines: models. (a) Mean temperature profiles, (b) Streamwise turbulent flux profiles, (c) Wall-normal turbulent heat flux profiles.

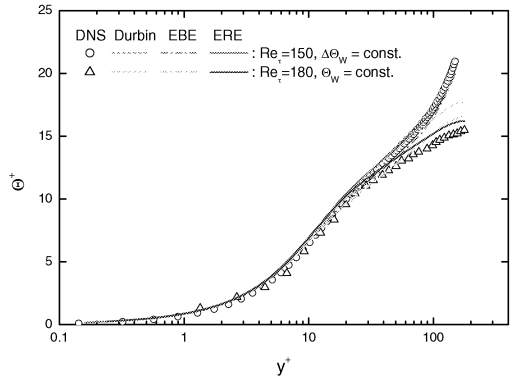

Fig. 2 Predicted heat transfer behaviour in a non-rotating channel with constant wall temperature boundary conditions. symbols: DNS(Kasagi, 2004; Kim & Moin, 1987), lines: models.

Rotating channel flows

Coriolis and centrifugal forces arising from imposed system rotation can substantially alter the mean flow, the intensity, the heat fluxes and the structure of turbulence. Second moment closure is the most natural level of turbulence model closure to account for rotation, because this modelling approach approves the appearance of the exact production terms due to mean flow gradients and system rotation. Thus, in order to test the prediction ability of a second moment closure, it is natural to consider the rotating channel flow with heat transfer. A sketch of the computational domain with constant temperature difference boundary condition is shown in Fig. 3. Cases SP and ST correspond to the rotation around spanwise and streamwise axes, respectively. When the channel rotates about a spanwise axis, Coriolis forces stabilize the turbulent flow near the leading(suction) wall and augments the turbulence near the trailing(pressure) wall(Kasagi, 2004). The streamwise rotating channel is a challenging flow field for a second moment turbulence closure, because, in comparison with the spanwise rotating, all six Reynolds components are non-zero. Thus, with the simple flow field relatively, we can decide whether a new second moment closure reproduces all Reynolds stress components satisfactorily or not.

Figure 4 shows the comparisons of mean velocity across the channel with the DNS data of Kasagi(2004) in spanwise and streamwise rotating channel flows at $Ro_\tau = 2.5$. The rotation number Ro_τ is defined using the channel width D, rotation rate Ω and the friction velocity u_τ. Although the some discrepancy is observed in central region of spanwise rotation profile, the predicted results due to the EBM of Thielen *et al.*(2004) are well reproduced comparatively in both rotating cases.

Figure 5 shows the predicted non-dimensional mean temperature and heat fluxes profiles across the channel. In this figure, SPR means spanwise rotation and STR streamwise rotation. The results due to the present ERE show better distributions than the other models in the rotating channel calculation. Especially, the predictions of mean temperature and streamwise heat flux with STR is very close to DNS (Kasagi, 2004). However, in case of SPR, the mean temperature is over-predicted in pressure side and under-predicted in suction side.

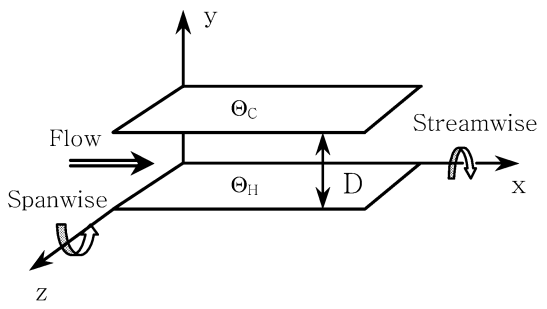

Fig. 3 Computational domain of rotating channel with heat transfer.

The discrepancy of non-dimensional temperature profile is induced from the under-predicted normal heat flux as shown in figure Fig. 5(c). Also, we can see that the streamwise heat flux in suction side of SPR is affected by wall-normal heat flux, which is relatively under predicted comparing to DNS.

Figure 6 shows the distributions of elliptic blending function ψ^2, which is adopted in the present EBE model only, across the rotating channel.

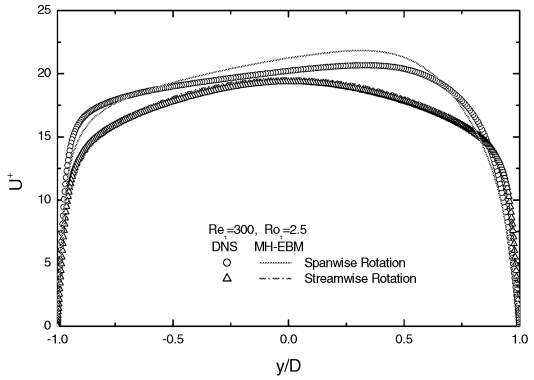

Fig. 4 Predicted streamwise velocity behaviour in rotating channels at $Re_\tau = 300$ and $Ro_\tau = 2.5$. symbols: DNS(Kasagi, 2004), lines: EBM (Thielen *et al.*, 2005)

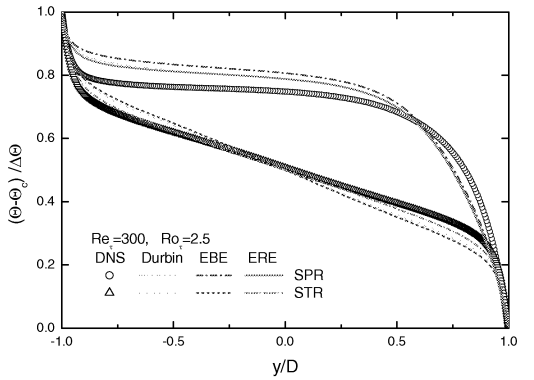

(a)

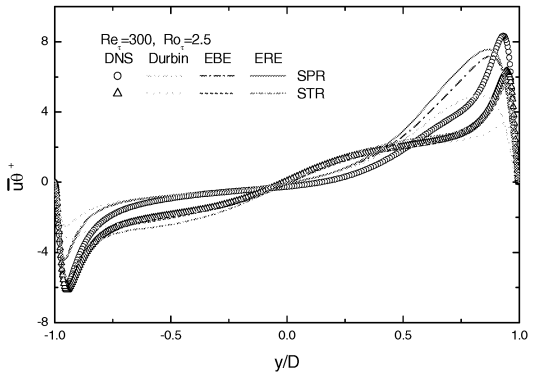

(b)

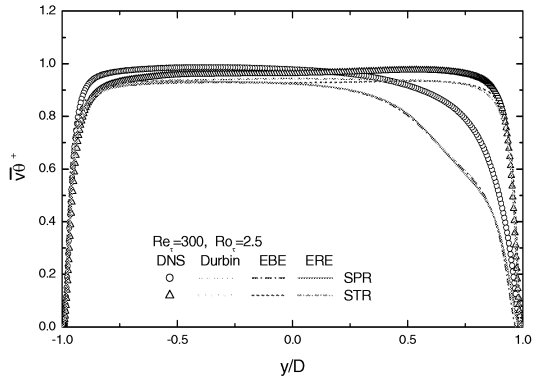

(c)

Fig. 5 Summary of predicted heat transfer behaviour in rotating channels at $Re_\tau = 300$ and $Ro_\tau = 2.5$. symbols: DNS(Kasagi, 2004), lines: models. (a) Non-dimensional mean temperature profiles. (b) Streamwise heat flux profiles. (c) Wall-normal heat flux profiles.

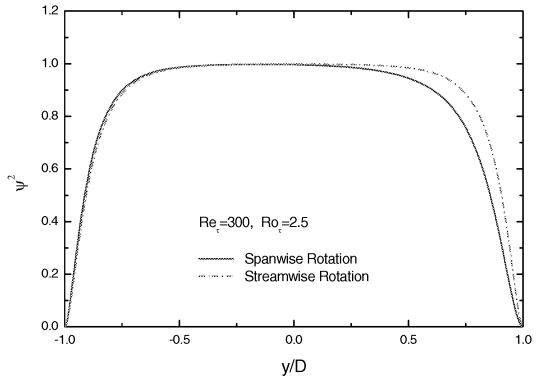

Fig. 6 Distributions of elliptic blending function ψ^2 across the channel at $Re_\tau = 300$ and $Ro_\tau = 2.5$.

We can see that the effect of spanwise rotation is reflected on the ψ^2. That is, the collapsed distribution of ψ^2 in suction side is correspond to the position of relaminarlization in the mean velocity.

Rotating square duct flows

In order to test the present elliptic concept heat flux models in three dimensional flow with heat transfer, as shown in Fig. 7, the rotating square duct flows with constant wall heat flux (CWH) and constant wall temperature (CWT) boundary conditions are adopted in $Re_\tau = 300$ and $Ro_\tau = 1.5$. In Fig. 7, y_{cb} means coner bisector and y_{wb} wall bisector. If a square duct is subjected to system rotation, the pressure gradient which arise to balance the Coriolis force gives rise to secondary fluid motion in cross section of duct. That is, the formation of pairs of counter-rotating longitudinal vortices may occur in square duct flows. If the rotation vector is perpendicular to the streamwise flow and parallel to one pair of walls, the Coriolis forces induce a pressure gradient perpendicular to these walls. The pressure field due to the rotational effect thus produces a flow along the other pair of walls, from the pressure side to the suction side (Pettersson & Adersson, 2003). It is well known that the turbulent mixing of fluid particles is enhanced in the regions of flow where the stratification of the streamwise momentum is unstable with respect to the Coriolis force (pressure side), whereas mixing is reduced where the stratification of the streamwise momentum is stable (suction side) (Pallares & Davidson, 2002).

Figure 8 shows the prediction pattern of secondary flow in x-y cross section with respect to Thielen *et al.*'s EBM in comparison with LES (Pallares & Davidson, 2002). In this figure, we can see how turbulence-driven secondary flows are affected by rotational effect and, that the secondary flow field is consisted of two large and two small counter rotating cells. The mean streamwise velocity contours reveal a fairly wide region in the central part of the duct in both EBM and LES simulations. Except the position of small cell occurring at the top near wall and the shape of maximum contour of streamwise velocity, the flow pattern with respect to Thielen et al.'s EBM is very similar to that of LES. That is, from the prediction of flow field due to the EBM, we can assess that the prediction performance of EBM is close to the LES in the square duct at least.

It can be seen in Fig. 9 that the predictions due to the present EBE and ERE models are plotted in comparison with LES (Pallares & Davidson, 2002). The temperatures in Fig. 9 are non-dimensionalized to $\Theta = (T - \langle T \rangle_w)/T_\tau$. T_τ is the friction temperature and $\langle T \rangle_w$ is the peripherally averaged wall temperature. A constant wall temperature, $\Theta_w = 0$ is imposed to at the four walls when the CWT boundary conditions is given, while a constant value of the wall heat flux is used for the thermal boundary condition CWH.

The position of minimum temperature occurs in the position of the maximum streamwise velocity component with CWT boundary condition in all simulations. As shown in Fig 9, temperatures are higher on the stable side where the effect of rotation is stabilizing. Also, the mean temperature contour patterns with CWT boundary conditions is very similar to that of streamwise mean velocity, in especially ERE prediction. That is, the contours of temperature corresponding to the CWT boundary condition (solid lines) are, like the streamwise velocity contours, stratified in the central part of the duct, which indicates the absence of heat transfer along the x direction. Accordingly, the forced convection with CWT boundary condition is directly affected by the flow field. On the other hand, the CWH thermal field (dotted lines) has important temperature gradients in the x direction. However, we can see that the discrepancy in the patterns of minimum contours is existed in between the present models and LES. The separated contours in the duct are reproduced by the present models, which is not shown in LES. In the present predictions, as can be seen in Fig. 9(b), the temperature contours due to ERE is relatively close to LES.

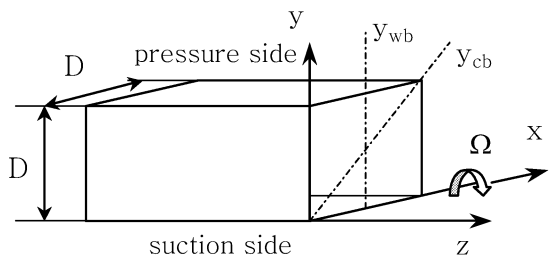

Fig. 7 Computational domain of rotating square duct flow with heat transfer.

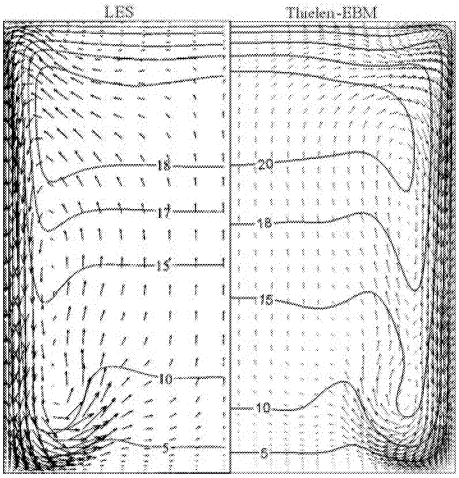

Fig. 8 Predicted streamwise velocity contours in a rotating square duct at $Re_\tau = 300$ and $Ro_\tau = 1.5$.

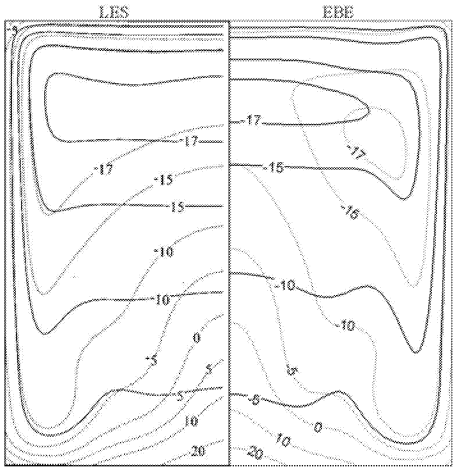

(a)

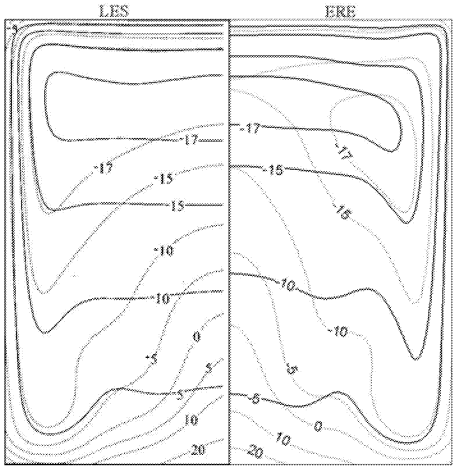

(b)

Fig. 9 Predicted mean temperature contours in a rotating square duct at $Re_\tau = 300$ and $Ro_\tau = 1.5$. solid lines: CWT boundary condition, dotted lines: CWH boundary condition. (a)EBE, (b)ERE.

CONCLUSIONS

The appropriateness of the present second moment heat flux closures is examined by comparing the prediction results with the DNS and LES data. The distributions of wall normal heat flux across the spanwise rotation channel with respect to the present models are not satisfactory in comparison with the DNS, but, in the spanwise and streamwise rotating channel flows, the present models catch properly the effects of Coriolis forces on the temperature and heat flux profiles according to the rotation direction. In the rotating square duct, although the temperature profiles with respect to the present ERE model is close to the LES in both CWT and CWH boundary conditions, the reliable DNS study is required to assess the present models. However, the overall results presented in the present article are in resonable agreement with the DNS and LES data, giving confidence the present models can be applied to the industrial flows with heat transfer.

Acknowledgement

This work was supported by Korea Science & Engineering Foundation (Grant No. R05-2003-000-12391 -0).

REFERENCES

Nagano, Y. and Hattori, H. 2003, *J. Turbulence*, Vol. 4, 010.

Lai, Y.G. and So, R.M.C., 1990, *Int. J. Heat Mass Transfer,* Vol. 33, pp. 1429-1440.

Durbin, P.A., 1993, *J. Fluid Mech.*, Vol. 249, pp. 465-498.

Thielen, L., Hanjalic, K. Jonker, H. and Manceau, R. 2005, *Int. J. Heat Mass Transfer,* Vol. 48, pp. 1583-1598.

Kawamura, H, 2004, DNS database in "http://murasun.me.noda.tus.ac.jp/"

Kasagi, N, 2004, DNS database in "http://www.thtlab.t.u-tokyo.ac.jp/"

Kim, J. and Moin, P., 1987, *Proceedings of the 6th Symposium on Turbulent Shear Flows,* 5-2.

Pettersson Reif, B.A. and Andersson, H.I., 2003, *J. Turbulence*, Vol. 4, 012.

Pallares, J. and Davidson, L, 2002, *Phys. Fluids*, Vol. 14, pp. 2804-2816.